0038-075X/04/16906-401–412
Soil Science

June 2004
Vol. 169, No. 6
Printed in U.S.A.

TECHNICAL ARTICLES

BORON TRANSPORT WITHIN AN AGRICULTURAL FIELD: UNIFORM FLOW VERSUS MOBILE-IMMOBILE WATER MODEL SIMULATIONS

P. J. Vaughan[1], P. J. Shouse[1], S. Goldberg[1], D. L. Suarez[1], and J. E. Ayars[2]

The transport of boron in soil is important to agriculture because boron concentrations in soil water are beneficial to plants only over a limited range (0.37 to 1.39 mmol L^{-1} for tolerant crops). Irrigation water in the San Joaquin Valley, California, commonly has elevated B concentrations, and soil water B can reach phytotoxic levels as a result of the concentrating effects of evapotranspiration. Because the constant capacitance model was successful in computing B speciation in soil water and on mineral surfaces, it was incorporated into a multicomponent solute transport code, and a 2-year field test of the model was performed for 43 sites within a 65-ha field in the San Joaquin Valley. The model predicted the adsorbed B ($XOB(OH)_3^-$) concentration successfully with a median scaled root mean square error (SRMSE) of 11% for 43 sites. The median SRMSE was 36% for prediction of total B and 46% for solution B. The higher SRMSE for solution B may be caused by lack of detail in specifying the lower boundary condition. A steady increase in SRMSE from east to west in the field, the same trend as the seven tile drains, suggests an unknown E-W systematic variation in the lower boundary condition. A mobile-immobile water transport model failed to exhibit significant improvement over the standard uniform flow model (UFM) and, thus, the simpler UFM was preferred. The change in total B mass at all sites generated was accurately predicted with a relative error of only 4.1%. This work has potential practical application in the study of the effect of water management practices on soil B. (Soil Science 2004;169:401–412)

Key words: Boron, transport, field simulation, Unsatchem, constant capacitance model, mobile-immobile model.

THERE is a restricted range of boron concentration in soil water that is beneficial to plants. At lower concentrations, plants exhibit boron deficiency, whereas at higher concentration, phytotoxicity occurs. The specific range of favorable response varies by species but has been characterized as 0.028 to 0.093 mmol L^{-1} for sensitive crops and 0.37 to 1.39 mmol L^{-1} for tolerant crops (Keren and Bingham, 1985). Plants respond to soil water boron concentrations rather than to adsorbed concentrations (Keren et al., 1985). Thus, development of management practices should consider maintenance of beneficial boron concentration in soil water. In California, the total yearly discharge of boron from water districts utilizing the San Joaquin river as the ultimate collector of drainage water is regulated; hence, another goal is reduction of boron dis-

[1]George E. Brown, Jr. Salinity Laboratory, USDA-ARS, 450 W. Big Springs Road, Riverside, CA 92507. Dr. Vaughan is corresponding author: E-mail: pvaughan@ussl.ars.usda.gov

[2]Water Management Research Laboratory, USDA-ARS, 9611 S Riverbend Ave., Parlier, CA 93648

Received Nov. 24, 2003; accepted March 11, 2004.

DOI: 10.1097/01.ss.0000131230.35979.b9

charge. These two goals — maintaining acceptable soil water boron concentrations while minimizing boron discharge from tile drains — represent potentially competing interests and reflect the difficulty in defining optimal boron management practices. This paper is concerned with modeling transport of boron in field conditions utilizing a one-dimensional, finite-element solution of the 1-D Richards equation for variably saturated water flow and the convection-dispersion equation for chemical transport (Simunek et al., 1996; Suarez and Simunek, 1997).

Boron sorption has been described by Langmuir and Freundlich adsorption isotherms (Hatcher and Bower, 1958; Rhoades et al., 1970; Elrashidi and O'Connor, 1982; Perkins, 1995). These empirical isotherms can provide a representation of the equilibrium between adsorbed and solution species, but they have no pH dependence. Adsorbed B in soils increases with increasing pH in the range pH = 3–9 (Bingham et al., 1971; Keren et al., 1985; Goldberg, 1997). The pH dependence of boron sorption is significant to the transport of boron because solution pH may vary with location, depth, and time. The constant capacitance model provides a mechanistic representation of the B sorption reactions that is a better choice to manage the range of environmental conditions that may be encountered in B transport modeling because it considers the pH variable (Goldberg et al., 2000).

Corwin et al. (1999) identified the factors pH, ionic strength, and temperature as important to B transport modeling in a lysimeter. Utilizing a functional modeling approach and several different representations of the adsorption isotherm, they determined that the Keren model of boron adsorption provided the best model performance. This was attributed to the inclusion of pH and ionic strength dependence in the Keren model (Keren and Mezuman, 1981). The functional modeling approach of Corwin et al. (1999) required specification of the pH of soil water in advance, whereas the Unsatchem model can calculate pH and temperature internally (Simunek et al., 1996). The mechanistic approach would be a better choice for B transport modeling when sufficient data are available to adequately specify the model's requirements. For example, model predictions during application of soil amendments and green manuring could be especially advantageous due to the variation of soil water pH that may occur (Suarez, 2001).

The objective of this numerical modeling study was to evaluate simulations of B transport that utilized the constant capacitance model to predict sorption of B for field conditions. The numerical model, Unsatchem, was recently upgraded to treat preferential flow using the mobile-immobile water (MIM) approach for calculating solute transport (Coats and Smith, 1964; van Genuchten and Wierenga, 1976; Nkedi-Kizza et al., 1984; Al-Jabri et al., 2002). A study of Cl^- transport for the same data set as discussed here found that the MIM approach provided slightly better agreement between measured and predicted Cl^- concentrations than did the standard uniform flow model (UFM) (Vaughan, unpublished data, 2004). The Cl^- study provided estimates of MIM parameters that were utilized in computing some of the results reported here for B transport. In our implementation of the MIM model, the immobile water content was specified by

$$\theta_{im} = \theta_r + \eta(\theta_w - \theta_r) \quad (1)$$

where η is a dimensionless parameter varying between zero and one, θ_w is the volumetric water content, θ_r is residual water conten, and θ_{im} is the volumetric immobile water content (Vaughan et al., 2004). The mass transfer coefficient ω [T^{-1}] is defined by

$$\frac{\partial \theta_{im} c_{k,im}}{\partial t} = \omega(c_{k,m} - c_{k,im}) \quad (2)$$

which expresses the transfer rate of solutes between the two water fractions. In this equation $c_{k,m}$ is the concentration of the kth solute in the mobile liquid region and $c_{k,im}$ is the concentration in the immobile liquid region [mmol L^{-1}].

METHODS

Field Sampling

The field study was performed in a 65-ha field located in the Broadview Water District, San Joaquin Valley, California. The field study was a 2-year program of soil sampling and well depth measurements that began in November 1995. Soil sampling was conducted during the weeks beginning November 13, 1995, April 15, 1996, July 15, 1996, May 12, 1997, and November 10, 1997 on a 6 × 6 square grid with spacing of 140.4 m in N-S and E-W directions (Fig. 1). Nine other locations that had been studied previously for groundwater composition were also sampled. At each location, six soil samples were collected by a 0.05-m core sample tube in 0.3-m increments to a total depth of 1.8 m. Observation

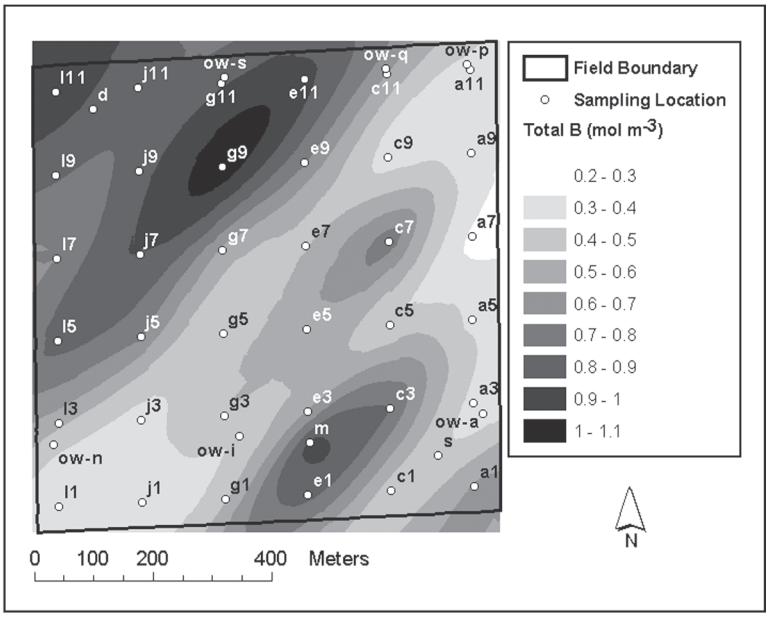

Fig. 1. Sampling locations and kriged surface of mean total resident B concentration for the depth range 0–1.8 m. Sampling took place in November 1997.

wells were located on the same grid and were installed during the crop growing seasons in 1996 and 1997. The wells provided depth-to-water measurements and groundwater samples for chemical analyses.

Boron Chemistry

The main goal of this study was to assess whether mechanistic modeling of boron transport could provide reasonably accurate predictions of changes in soil B over a 2-year period. The Unsatchem model was initially modified to predict B transport, with concentrations of aqueous and adsorbed B calculated from the constant capacitance model assuming a trigonal ($XOB(OH)_2$) form for the adsorbed B (Suarez and Simunek, 1997). The symbol "X" is used here to indicate surface species. Spectroscopic analysis determined that both a trigonal and a tetrahedral surface species ($XOB(OH)_3^-$) were present on the surface of an amorphous Al hydroxide (Su and Suarez, 1995). A study of 32 soils using the constant capacitance model suggested that B adsorption was better described as the tetrahedral ($XOB(OH)_3^-$) form (Goldberg et al., 2000). As part of the current work, the Unsatchem model was modified to calculate equilibrium between $XOB(OH)_3^-$ and solution species $B(OH)_3$ and $B(OH)_4^-$,

$$XOH_{(s)} + H^+_{(a)} \rightleftharpoons XOH^+_{2(s)} \quad (3)$$

$$XOH_{(s)} \rightleftharpoons XO^-_{(s)} + H^+_{(a)} \quad (4)$$

$$XOH_{(s)} + B(OH)_{3(a)} \rightleftharpoons XOB(OH)^-_{3(s)} + H^+_{(a)} \quad (5)$$

in which *s* represents surface and *a* aqueous species. The intrinsic equilibrium expressions for these reactions (Goldberg et al., 2000) are:

$$K^i_+ = \frac{[XOH^+_2]}{[XOH][H^+]} \exp(F\psi/RT) \quad (6)$$

$$K^i_- = \frac{[XO^-][H^+]}{[XOH]} \exp(-F\psi/RT) \quad (7)$$

$$K^i_{B-} = \frac{[XOH(OH)^-_3][H^+]}{[XOH][B(OH)_3]} \exp(-F\psi/RT) \quad (8)$$

where F is (Faraday constant, C mol_c^{-1}), ψ is (surface potential, V), R is (gas constant, J mol^{-1} $°K^{-1}$), and T is (temperature, °K). The square brackets represent concentrations (mol L^{-1}). K_+^i is the intrinsic surface protonation reaction constant, K_-^i is the intrinsic surface dissociation reaction constant, and K_{B-}^i is the surface complexation constant for the tetrahedral B species $XOB(OH)_3^-$. Solid-phase activity coefficients are

accounted for in the exponential terms (Goldberg et al., 2000). Additional constraints required to solve these equations are provided by mole balance of the surface sites and boron:

$$[XOH]_T = [XOH] + [XOH_2^+] + [XO^-] + [XOB(OH)_3^-] \quad (9)$$

$$[B_T] = [B(OH)_3] + [B(OH)_4^-] + [XOB(OH)_3^-] \quad (10)$$

Charge balance on the surface includes the negatively charged tetrahedral B species

$$\sigma = [XOH_2^+] - [XO^-] - [XOB(OH)_3^-] \quad (11)$$

where σ is the net surface charge (mol L^{-1}). Surface potential (ψ) is related to surface charge by $\sigma = CS_A a\psi/F$ where C is the capacitance density (F m^{-2}), S_A is the specific surface area ($m^2 g^{-1}$), and a is the suspension density (g L^{-1}). The solution speciation between $B(OH)_3$ and the tetrahedral borate anion, $B(OH)_4^-$, was calculated from the equilibrium expression

$$K_a = \frac{(B(OH)_4^-)(H^+)}{(B(OH)_3)(H_2O)} \quad (12)$$

where K_a is the acid ionization constant. Combining Eqs. (6) through (12) results in a pair of nonlinear equations and two unknowns, $[XOH_2^+]$ and $[XO^-]$. These two equations were solved numerically using a modified Newton-Raphson technique with an analytical Jacobian matrix. This numerical solution was included in the Unsatchem transport model.

Using the assumption that the surface species was $XOB(OH)_3^-$, a set of empirical relationships (Goldberg et al., 2000) was developed for predicting the intrinsic equilibrium constants defined by Eqs. (6) through (8). The Unsatchem program was modified to include these empirical relationships. Intrinsic equilibrium constants were estimated from commonly measured soil properties, including specific surface area (S_A), organic, and inorganic carbon contents (OC and IOC) and Al concentration. These properties represent important sinks for B adsorption in soils that are primarily clay, organic matter, and calcite (Goldberg et al., 2000).

$$\ln(K_+) = 7.852 - 0.102\ln(OC) - 0.198\ln(IOC) - 0.622\ln(Al) \quad (13)$$

$$\ln(K_-) = -11.967 + 0.302\ln(OC) + 0.058\ln(IOC) + 0.302\ln(Al) \quad (14)$$

$$\ln(K_{B-}) = -9.136 + 0.375\ln(S_A) + 0.167\ln(OC) + 0.111\ln(IOC) + 0.466\ln(Al) \quad (15)$$

Al, *OC*, and *IOC* are expressed as mass fractions (g kg^{-1} soil), and the units for S_A are $m^2 g^{-1}$. For this work, the field was resampled in 2001 at five of the original locations selected because they represented a large range of soil texture. *Al*, *OC*, and *IOC* and S_A were measured only for 29 samples collected at these locations in 2001. A regression analysis was performed to develop prediction equations for *Al*, *OC*, and *IOC* and S_A using clay and/or sand content and/or depth as independent variables. For the remaining 40 locations, these properties were estimated from the prediction equations.

Soil Chemical Analysis

Extracts were taken from both soil pastes of 1:1 water to soil ratio by mass and saturation pastes at room temperature (~22 °C) using deionized water. The extracts were analyzed for various elements, including Ca, Mg, Na, K, S, and B using inductively coupled plasma (ICP) emission spectrometry. This provided a complete set of solution B concentrations for two different water contents for all samples.

Specification of the initial conditions for B required both the *in situ* solution B concentration and the adsorbed concentration. B_{sw} is defined here as the solution B concentration at volumetric water content, θ_w. B_{sw} was calculated using

$$B_{sw} = \frac{\rho_b(B_{s1:1}V_{1:1}/m_s + B_{a1:1})}{\theta_w + \rho_b K_d} \quad (16)$$

where $V_{1:1}$ = total volume of water in the sample after the 1:1 dilution; m_s = dry soil mass; $B_{s1:1}$ = measured solution B [mmol L^{-1}], $B_{a1:1}$ = estimated adsorbed B concentration [mol Mg^{-1}]; ρ_b = bulk density [Mg m^{-3}]; and K_d = a function estimated from clay content and gravimetric water content [m^3 Mg^{-1}]. The ratio $V_{1:1}/m_s$ was required in this equation because most of the dilutions were not precisely 1:1. Similar equations have been applied to variation in boron desorption with varying water content (Tanji, 1970; Jame et al., 1982; Perkins, 1995). Initial solution B for each soil sample was calculated from Eq. (16) once the K_d function had been specified and $B_{a1:1}$ was calculated.

In order to obtain the K_d function for the 29 samples taken in 2001, the total B concentrations were determined as the sum of all B removed during six successive extractions. The adsorbed B concentration for both 1:1 and saturation paste extracts was then calculated as the difference between total B concentration and the solution B concentration. The estimation method for the $B_{a1:1}$ concentrations was tested by plotting the K_d function estimate of the $B_{a1:1}$ values for the 29 samples taken in 2001 against the measured values (Fig. 2).

The first step in generating the K_d function was linear curve fitting to predict the adsorbed concentrations for both the 1:1 and saturation paste extracts for the 29 samples taken in 2001 (Fig. 3). A linear relationship provided good fits to both sets of data and generated K_d values representing both water contents. The units were g Mg^{-1} soil for

$$B_{ads} = K_d B_{sol} \tag{17}$$

adsorbed concentration (B_{ads}) and mg L^{-1} for the aqueous concentration (B_{sol}).

Clay minerals provide sites for boron adsorption (Goldberg, 1999) and, in the field studied here, clay content varied substantially ($6.3 \leq$ clay% ≤ 65.0). Thus, clay content was one important variable in the K_d function. The other was gravimetric water content. Various parametric K_d functions, $K_d = K_d(\%clay)\theta_g$ were tested in an effort to obtain a reasonably good fit to the data.

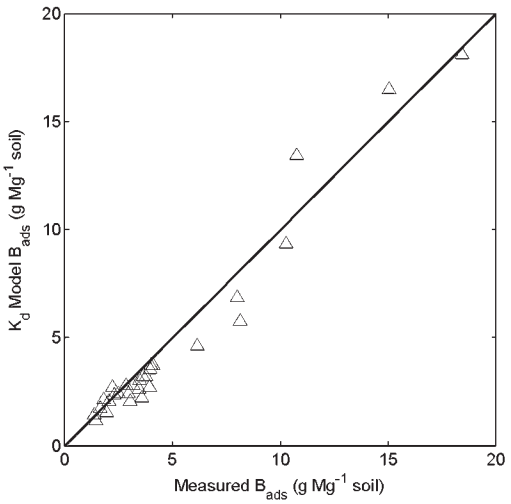

Fig. 2. Adsorbed B calculated from the K_d function compared with measured values.

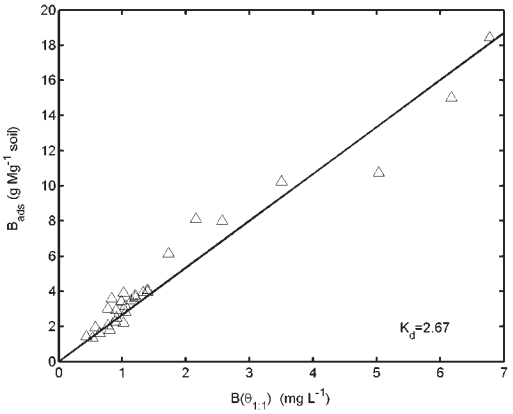

Fig. 3. Adsorbed B vs. Solution B for 1:1 extractions of 29 samples taken at five locations.

$$K_d = \frac{a\theta_g}{b+\theta_g} \tag{18}$$

We found that a set of nonlinear functions with parameters a and b for five different ranges of clay content provided an adequate representation (Eq. 18). As a soil dries out, boron species in soil solution become more concentrated, and the constant capacitance model predicts decreasing K_d (Vaughan and Suarez, 2003). However, the exact variation in the distribution of B between adsorbed and solution species as water content approaches zero is unknown. Therefore, it would not be appropriate to estimate K_d from Eq. (18) for $\theta_g < 0.05$. The range of measured water contents for the field in November 1995 was $\theta_g =$ 0.053 to 0.505.

K_d and θ_g pairs were selected for each of five ranges of clay content (0–0.2, 0.2–0.3, 0.3–0.4, 0.4–0.5, >0.5). Extrapolation of $K_d(\theta_g, \%clay)$ to the field volumetric water content using Eq. (18) generated estimates of the initial aqueous and adsorbed boron concentrations from measurement of the 1:1 solution concentration. Despite substantial variation in texture within the 65-ha field, variation of the clay mineralogy was probably small. The K_d function may, therefore, be applied to data sets obtained from this field but would not necessarily apply to data sets from other locations.

Hydraulic Properties

Particle size analysis was performed on six, 40-g soil samples from each of 45 locations. The sand fraction was determined by sieving, the silt

and clay fractions by the hydrometer method. Bulk density was determined for soil cores that were 0.05 m diameter and 0.3 m in length. The soil was dried at 100 °C until no further weight change occurred. The water retention parameters, including saturated water content, residual water content, and the parameters α and n (van Genuchten, 1980), were estimated using the Rosetta computer program (Schaap et al., 1998). This estimate was based on bulk density and texture as determined by particle size analyses performed for samples from 20 locations and six depths. Saturated hydraulic conductivity was also estimated using the Rosetta program.

Finite-Element Model

The model simulated water flow and boron transport at 45 locations in the field (Fig. 1). Other processes simulated were heat transport, CO_2 transport, multicomponent chemical transport, plant root water uptake, and root growth. All of these processes are potentially significant to B transport. Water flow was calculated by a finite-element numerical solution of the Richards equation (Simunek et al., 1996). Chemical transport was represented either by the convection-dispersion equation (CDE) or the mobile-immobile model (MIM) of solute transport (van Genuchten and Wierenga, 1976). The standard CDE simulations assume a single-valued water velocity at any specified depth and time and are called uniform flow model simulations (UFM). Equilibrium concentrations were recalculated for each finite element that experienced a non-negligible change in solute concentration during the previous time step. The vertical finite-element column at each location was 3 m in length and consisted of 377 elements. Element thickness varied exponentially from 3.0×10^{-3} m at the top to 0.03 m at a depth of 2.7 m. Below this depth, element thickness decreased linearly so as to maintain stability of the calculations near the base of the column.

Field Crops

The field was cropped to tomato (*Lycopersicon lycopersicum* L.) in 1996 and cotton (*Gossypium hirsutum* L.) in 1997. Both crops were furrow-irrigated, with water supplied to tomato by gated-pipe and to cotton by siphon tube. Crop modeling included root growth and root water uptake controlled by water and salinity stress functions (Simunek et al., 1996).

Boundary Conditions

At the soil surface, the atmospheric boundary condition for water flow was applied and external atmospheric conditions controlled the boundary condition, which may alternate between time-dependent prescribed flux (m d^{-1}) and, if ponding occurred, prescribed pressure head (m) (Simunek et al., 1996). Ponding was permitted to a maximum depth of 0.05 m that was never exceeded in the simulations. Precipitation records obtained from the Broadview Water District central office were combined with irrigation data for the field, thus building a continuous record of potential soil surface water flux for the 2-year simulation period starting November 1, 1995. The predicted actual surface flux and the possible development of ponding or runoff were determined during the simulations.

The Unsatchem model requires specification of a minimum critical value for the water pressure head at the upper boundary in order to preserve numerical stability in the chemical speciation calculations. Potential soil surface evaporation was specified that would meet this constraint and still provide for drying of the soil after precipitation or irrigation events. The lower boundary of the simulated profile was located 3 m below the soil surface. Pressure heads at this boundary were determined from depth-to-water records for Water Management Research Laboratory (WMRL) wells installed at the soil sampling locations.

Specified temperature boundary conditions were applied at both the soil surface and at a 3-m depth. Surface temperature was approximated as a diurnal sinusoidal variation, with an amplitude of 5 °C around the mean daily air temperature supplied by California Irrigation Management Information System (CIMIS) weather records. The CIMIS station was located 20 km northwest of the field. The specified temperature at the 3-m depth was a constant 15 °C. Temperatures along the finite-element column were calculated by the heat transport model.

In addition to solute transport, the Unsatchem model also calculates CO_2 production and transport in both the air and water phases (Simunek et al., 1996). The CO_2 concentration in the water phase is important in this study because of its effect on the pH and alkalinity of soil water in a calcareous soil. As noted above, pH affects B adsorption strongly. A standard set of parameter values for CO_2 production and transport was applied (Suarez and Simunek, 1993). The lower boundary condition in their study was zero flux at 5 m depth. The range of volumetric CO_2 concentrations at 2 m depth for a variety of CO_2 production rates, water flow conditions, and depth distributions of CO_2 production was

0.005–0.05 (Suarez and Simunek, 1993). We have no field measurements of soil CO_2 concentration, and, therefore, we estimated the CO_2 concentration at the lower boundary (3 m) of the modeled profile as 0.02. The CO_2 concentration at the soil surface was set to 3.65×10^{-4}, the approximate atmospheric concentration.

Initial Conditions

The initial conditions other than B concentrations included water content, CO_2 concentration, temperature, and concentrations for solution species. The simulation started on November 1, 1995, a time of year when San Joaquin Valley soils normally exhibit low water content. Gravimetric soil water contents were measured on the basis of water loss at 100 °C for all soil samples taken in the week starting November 13, 1995. These measurements approximate closely the water content on November 1 because of a lack of irrigation or precipitation during the intervening period. Volumetric water contents required by the model were calculated from the gravimetric values and the measured bulk density. Initial soil CO_2 concentration was assumed to be atmospheric at the surface increasing linearly to 0.018 at 1.65 m depth and then increasing linearly to 0.02 at 3 m depth. The initial temperature was set to a constant 15 °C at all depths. The initial concentrations of solution species other than B were estimated from the measured 1:1 values recalculated to the *in situ* water content.

Model Evaluation

The scaled root mean square error,

$$SRMSE = \frac{100}{\bar{O}} \sqrt{\frac{\sum (P_i - O_i)^2}{N}} \qquad (19)$$

represented the discrepancy between model predictions and measured concentrations, where P_i are model predictions, O_i are observations, and $\bar{O}$ is the arithmetic mean of N observations (Vanclooster et al., 2000).

MIM Parameter Values

A parallel study of Cl^- transport for the same field and the same time period determined optimal values for the MIM model parameters ω and η as defined by Eqs. (1) and (2). Simulations were performed for a systematic variation of the two parameters over the ranges: $10^{-2} \leq \omega \leq 10^{-4}$ and $0.0 \leq \eta \leq 0.25$ (Vaughan, unpublished data, 2004). The SRMSE was calculated considering Cl^- data from four different sampling periods between April, 1996 and November 1997. These calculations were performed successfully for 33 locations on the 6×6 square grid. The results indicated that the MIM provided better agreement for low values of ω and/or high values of η at 64% of the 33 locations on the grid. At the remaining 36%, the MIM did not represent an improvement on the UFM for prediction of Cl^- profiles. Based on these results and similar tests at eight other locations, we selected MIM parameter values for 41 locations where MIM simulations were successful.

Numerical Accuracy of the Model

The Unsatchem model calculates mass balance for all species as a check on the transport model. Although this is not a complete test of numerical accuracy, it is a necessary condition and assures us that the mass balance error calculated from measured values and model results is not caused simply by failure of numerical approximations. For the purpose of computing mass balance error, the true value for total B mass is the sum of the time integrals of the fluxes at the top and bottom of the column plus the initial total B mass:

$$m_t = \int_0^t q_t dt + \int_0^t q_b dt + \int_{-L}^0 (B_{sol,i}\theta_w + B_{ads,i}\rho_b) dz \qquad (20)$$

where m_t is the mass of B in the column at time t (mol), and q_t and q_b are the fluxes of B at the upper and lower boundaries (mol m^{-2} d^{-1}). L is the depth of the modeled profile (m). $B_{sol,i}$ (mol L^{-1}) and $B_{ads,i}$ (mol Mg^{-1}) are the initial solution and adsorbed B concentrations. $B_{sol,t}$ and $B_{ads,t}$ are the concentrations at time t.

$$m_c = \int_{-L}^0 (B_{sol,t}\theta_w + B_{ads,t}\rho_b) dz \qquad (21)$$

$$\varepsilon_c = 100 * \frac{|m_t - m_c|}{m_t} \qquad (22)$$

The computed B mass in the column, m_c, at time t is given by a numerical summation approximating Eq. (21). The relative error ε_r (percent) is given by Eq. (22). For the UFM, the mean relative error for 43 locations was 2.2%, and the range was [0.6%, 4.2%]. While this is not ideal, it is small compared with other sources of error discussed later.

RESULTS AND DISCUSSION

Two model types were evaluated for their predictive capability. The standard uniform flow (UFM) assumes that only one water velocity profile exists at any given time. The mobile-immobile water flow model (MIM) separates soil water into mobile and immobile liquid regions, thus creating both a finite and a zero velocity profile. A qualitative comparison suggests that the model tends to smooth out the total B concentrations relative to the measured values. The measured total B surface was generated by point kriging utilizing a linear combination of an anisotropic semivariogram model and an isotropic model (Fig. 1).

For the UFM, profiles of the adsorbed and total B concentrations for location m in November, 1997 provided good agreement with the adsorbed and total B concentrations calculated from the 1:1 extracts (Fig. 4). The UFM performed poorly at location e1 (Fig. 5). The agreement of model and data for the remaining 41 locations varied between the two extremes (Figs. 4 and 5). Model predictions of the total mass of B for November 1997 in the top 1.8 m of the profile exceeded measured values at 24 locations and were lower at the remaining 19. The standard deviation of model predicted and measured value for the total B concentration at all depths and all locations was 0.25 mol m^{-3}, and the mean measured total B concentration was 0.61 mol m^{-3} (CV = 42%).

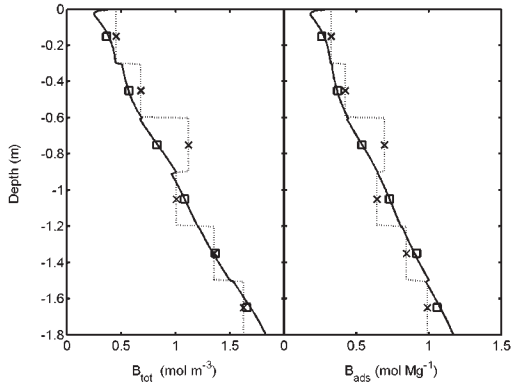

Fig. 4. Profiles of total and adsorbed B for location "m" where a good match between model and data was obtained. Solid line is UFM result for November 1997 with squares indicating mean value for each sampling depth range. Dashed lines and x symbols represent B concentrations estimated from the measured 1:1 B concentration data.

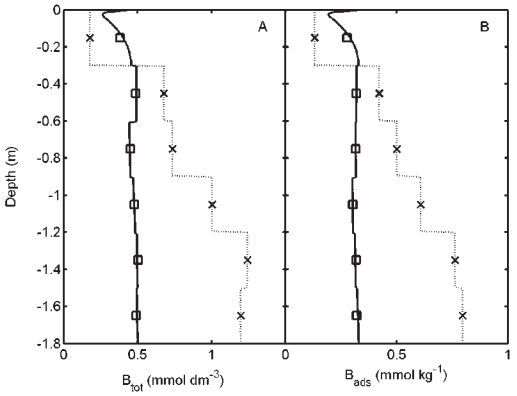

Fig. 5. Profiles of total and adsorbed B for UFM simulation at "e1", a location where both the UFM and MIM performed poorly. Symbols are the same as in Fig. 4.

The spatial distribution of total B concentration calculated by the UFM is similar to the spatial distribution of measured values, with maxima and minima occurring in approximately the same areas (Figs. 1 and 6). A significant difference in the two maps is the distinct SW-NE trend in the shapes of features (Fig. 1). This was due to a pronounced anisotropy in the semivariogram for the measured total B concentrations that was also present, but greatly reduced, in the UFM calculated results (Fig. 6).

The MIM performance was very similar to that of the UFM. At 20 of the 41 locations where simulations were successful, the model prediction of the total B mass exceeded the measured value. The standard deviation was 0.26 mol m^{-3}, which is almost identical to the value obtained for the UFM, so there was no significant improvement in the prediction of the total mass of B at each location by the MIM.

Instability in the transport calculations at high mobile water velocity limited the range of η parameter values that could be studied; thus, the values obtained for ω and η were probably not optimal. For a set of 41 locations where complete sets of MIM simulations were conducted successfully for systematically varied parameter values, 54% of the locations showed minima in SRMSE for $\eta = 0.25$, the maximum value. For 38% of these locations, the minima in SRMSE occurred when $\eta = 0.0$. Likewise, the optimal values of ω were 10^{-4} at 28% of these locations and 10^{-2} at 51%. This suggests very little consistency in the optimal MIM parameter values and is further evidence that the MIM did not provide a significant improvement over the UFM.

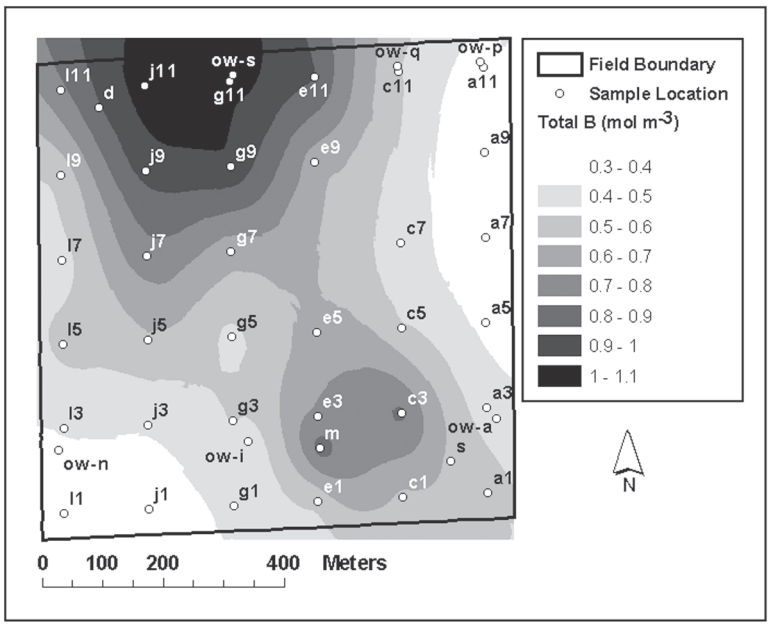

Fig. 6. Mean total resident B concentration for the depth range 0–1.8 m calculated by the UFM for November, 1997.

The ability of the model to represent changes in the total amount of B present can be assessed by calculating the total mass of B for 43 model columns (each column area = 10^{-4} m^2, for length units specified as cm). For the depth range 0–1.8 m, the UFM calculation of total B present was 4.55 mmol. Based on concentrations estimated from the November 1997 sampling, the measured total B was 4.74 mmol for a relative error of 4.1%. For the 41 locations where MIM simulations could be completed, the computed total mass was 4.18 mmol and the measured mass was 4.44 mmol. The relative error was 5.9% implying a slightly improved performance for the UFM with respect to changes in total B. We do not know precisely why the simulations failed at a few locations, but the large step changes in hydraulic properties between adjacent layers seems to be a contributing factor.

The SRMSE for total B was substantially larger than the SRMSE for adsorbed B (Fig. 7). Therefore, the model prediction of solution B ($B(OH)_3 + B(OH)_4^-$) has a greater error than the prediction of adsorbed B. The greater SRMSE for solution B, as compared with adsorbed B, is consistent model prediction of Cl^- leaching in this field, which was greater than actually occurred (Vaughan, unpublished data, 2004). The SRMSE for each location was kriged using a point kriging method with an isotropic semivariogram model (Fig. 8). SRMSE generally increases westward in the field.

Relation to Previous Work

Studies of B adsorption on individual soil minerals and soils demonstrated the utility of the constant capacitance model (Goldberg, 1999; Goldberg et al., 2000). The constant capacitance model provides a mechanistic description of specific surface reactions that provide the rationale for variation of adsorption with pH. The approach provides a more generally applicable model than the various empirical models that have been used to represent B sorption. The cur-

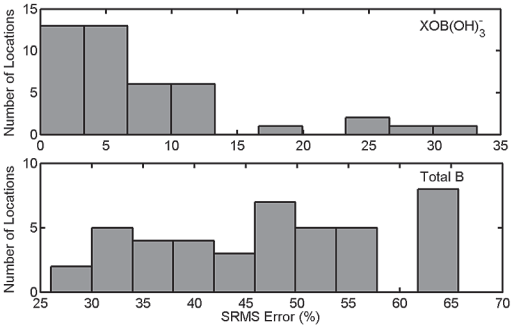

Fig. 7. Histograms of the SRMSE statistic for adsorbed B ($XOB(OH)_3^-$) and total B.

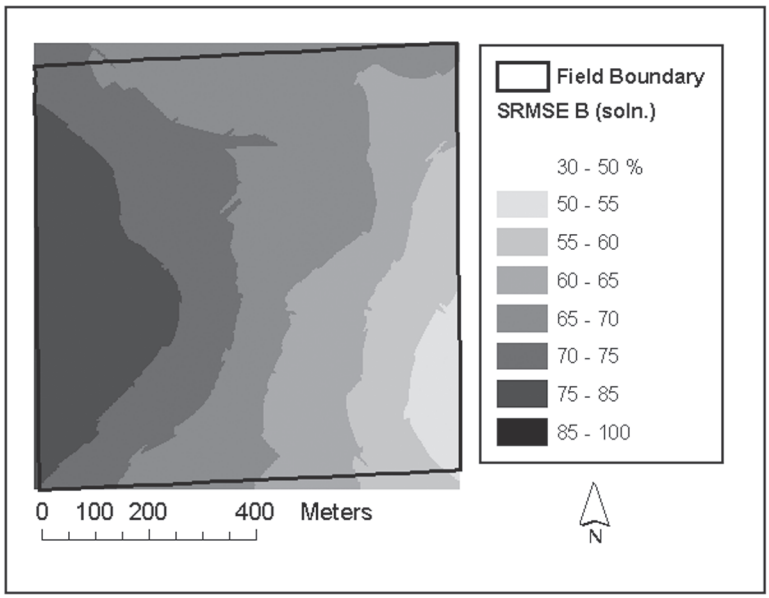

Fig. 8. Spatial variation of the SRMSE statistic representing error for solution B (UFM model).

rent work indicates that modeling of B transport for field conditions utilizing the constant capacitance model, with the assumption that all surface B is tetrahedral, was reasonably successful (Fig. 6). This study also provides some further justification for the use of the empirical equations predicting the intrinsic equilibrium constants (Eqs. 13–15, Goldberg et al., 2000).

MIM and UFM Results

The measured total B in soil columns was less than the UFM prediction at 24 of 43 locations, implying that the UFM did not predict enough leaching. The MIM, however, did not improve the result at these locations and, in fact, added to the retardation effect caused by the B adsorption and reduced the model prediction of B leaching. Thus, for these 24 locations the UFM would clearly be the best choice.

B leaching was overpredicted by the UFM for the remaining 19 locations. At these locations, the MIM was thought to possibly provide a better representation because of storage and the slow release of B from the immobile liquid regions. However, for these 19 locations, the MIM SRMSE = 37.9% for total B, whereas the UFM SRMSE = 37.2%, so there was no improvement obtained by using MIM to model B transport. Thus, there was no reason to consider the MIM to be an improvement over the UFM at either set of locations, making the UFM a better choice for B transport at all locations because it is simpler.

We found that the MIM was more suitable than the UFM for prediction of Cl^- transport at 64% of the locations (Vaughan, unpublished data, 2004). To the extent that Cl^- transport was better described by the MIM, the question arises as to why the UFM should be considered satisfactory for B transport. The answer lies in the time frame of the experiment. The 2-year period was sufficient for the UFM to generate significantly greater leaching of Cl^- than actually occurred. Therefore, the MIM improved predictions. But the 2-year period was not sufficient to expose the significant leaching of B due to the retardation effect of the sorption, so the UFM had sufficient predictive capability for the 2-year period.

Spatial Distribution of Model Error

Spatial distribution of SRMSE shows a consistent increase going westward in the field (Fig. 7). There are seven E-W trending tile drains, at 1.5–1.8-m depth, spaced 123 m apart, in which water normally flows eastward to a main drain running N-S along the eastern boundary. The lower boundary conditions directly affecting solute transport were Dirichlet conditions for pressure head and the solution B concentration. Specification of these conditions relied on well depth measurements and chemical analyses of well water samples. These measurements and analyses

were only conducted at regular intervals during the growing seasons when the wells were installed. Thus, there was considerable uncertainty concerning the lower boundary conditions, particularly during the winter when significant precipitation occurred. The consistent increase in SRMSE going westward in the field suggests that assumptions regarding the lower boundary conditions may have been reasonable near the eastern boundary of the field but were of consistently lower quality towards the west. This could be related to less leaching and decreasing leaching efficiency of drainage related to the E-W trend of the drains.

CONCLUSIONS

The field testing of the Unsatchem simulation of B transport demonstrated that the constant capacitance model of B speciation that was incorporated into the solute transport model worked well for predicting changes in the adsorbed B concentration over a 2-year period. For the UFM, the median SRMSE for adsorbed B was 11%. The median SRMSE was 36% for prediction of total B and 46% for solution B. The UFM simulations at 43 locations also accurately predicted the variation in total mass of B for all locations during the 2-year period (ϵ_r). The geographic distribution of the SRMSE for solution B can be characterized as increasing steadily from east to west in the field. This may be caused by increasing uncertainty in the specification of bottom boundary conditions for pressure head and/or solution B concentration that may be related to the leaching efficiency of tile drainage.

Results were obtained for both the UFM and the MIM. Values for the MIM parameters η and ω were assumed to be the optimal values obtained for chloride transport at each location. No significant improvement was obtained through use of the MIM for boron transport so the simpler UFM was judged to be the best choice. This conclusion applies only to the 2-year simulation performed here. It is likely that at locations where the model predicted a net desorption of B, the MIM would eventually prove a better choice. The results suggest that planning of field experiments to test the applicability of the UFM and the MIM for transport of sorbing species must consider the time required to differentiate between the two models.

This work is of importance to numerical modeling of solute transport in the vadose zone because it demonstrates transport modeling of B, including the constant capacitance model for simultaneous calculation of B adsorption and solution speciation. The model also has potential practical utility for those wishing to study the effects of agricultural water management practices on the movement of B in soil.

ACKNOWLEDGMENTS

The authors acknowledge work done by Richard Schoeneman and Richard Soppe of the USDA Water Management Research Laboratory in Fresno. We are grateful to David Cone of the Broadview Water District for providing records of irrigation, precipitation, and well depths. Salinity laboratory staff who assisted in this study were JoAn Fargerlund, Harry Forster, Jack Jobes, Nahid Vishteh, and Jim Wood.

REFERENCES

Al-Jabri, S. A., R. Horton, D. B. Jaynes, and A. Gaur. 2002. Field determination of soil hydraulic and chemical transport properties. Soil Sci. 167:353–367.

Bingham, F. T., A. L. Page, N. T. Coleman, and K. Flach. 1971. Boron adsorption characteristics of selected soils from Mexico and Hawaii. Soil Sci. Soc. Am. J. 35:546–550.

Coats, K. H., and B. D. Smith. 1964. Dead-end pore volume and dispersion in porous media. J. Soc. Pet. Eng. 4:73–84.

Corwin, D. L., S. Goldberg, and A. David. 1999. Evaluation of a functional model for simulating boron transport in soil. Soil Sci. 164:697–717.

Elrashidi, M. A., and G. A. O'Connor. 1982. Boron sorption and desorption in soils. Soil Sci. Soc. Am. J. 46:27–31.

Goldberg, S. 1997. Reactions of boron with soils. Plant Soil 193:35–48.

Goldberg, S. 1999. Reanalysis of Boron adsorption on soils and soil minerals using the constant capacitance model. Soil Sci. Soc. Am. J. 63:823–829.

Goldberg, S., S. M. Lesch, and D. L. Suarez. 2000. Predicting boron adsorption by soil using soil chemical parameters in the constant capacitance model. Soil Sci. Soc. Am. J. 64:1356–1362.

Hatcher, J. T., and C. A. Bower. 1958. Equilibria and dynamics of boron adsorption by soils. Soil Sci. 85:319–323.

Jame, Y. W., W. Nicholaichuk, A. J. Leyshon, and C. A. Campbell. 1982. Boron concentration in the soil solution under irrigation: A theoretical analysis. Can. J. Soil Sci. 62:461–470.

Keren, R., and F. T. Bingham. 1985. Boron in water, soils, and plants. Adv. Soil Sci. 1:229–276.

Keren, R., F. T. Bingham, and J. D. Rhoades. 1985. Plant uptake of boron as affected by boron distribution between liquid and solid phases in soil. Soil Sci. Soc. Am. J. 49:297–302.

Keren, R., and U. Mezuman. 1981. Boron adsorption by clay minerals using a phenomenological equation. Clays Clay Miner. 29:198–204.

Nkedi-Kizza, P., J. W. Biggar, H. M. Selim, M. Th. van Genuchten, P. J. Wierenga, J. M. Davidson, and D. R. Nielsen. 1984. On the equivalence of two conceptual models for describing ion exchange during transport through an aggregated Oxisol. Soil Sci. Soc. Am. J. 46:471–476.

Perkins, C. V. 1995. The consideration of soil boron adsorption and soil solution boron concentration as affected by moisture content. Geoderma 66:99–111.

Rhoades, J. D., R. D. Ingvalson, and J. T. Hatcher. 1970. Laboratory determination of leachable soil boron. Soil Sci. Soc. Am. Proc. 34:871–875.

Schaap, M. G., F. J. Leij, and M. Th van Genuchten. 1998. Neural network analysis for hierarchical prediction of soil water retention and saturated hydraulic conductivity. Soil Sci. Soc. Am. J. 62:847–855.

Simunek J., D. L. Suarez, and M. Sejna. 1996. The Unsatchem software package for simulating one-dimensional variably-saturated water flow, heat transport, carbon dioxide production and transport, and multicomponent solute transport with major ion equilibrium and kinetic chemistry, Version 2.0. Research Report No. 141. US Salinity Laboratory, Riverside, CA,

Su, C., and D. L. Suarez. 1995. Coordination of adsorbed boron: A FTIR spectroscopic study. Environ. Sci. Technol. 29:302–311.

Suarez, D. L. 2001. Sodic soil reclamation: Modelling and field study. Aust. J. Soil Res. 39:1225–1246.

Suarez, D. L., and J. Simunek. 1993. Modeling of carbon dioxide transport and production in soil: 2. Parameter selection, sensitivity analysis and comparison of model predictions to field data. Water Resour. Res. 29:499–513.

Suarez, D. L., and J. Simunek. 1997. Unsatchem: Unsaturated water and solute transport model with equilibrium and kinetic chemistry. Soil Sci. Soc. Am. J. 61:1633–1646.

Tanji, K. K. 1970. A computer analysis on the leaching of boron from stratified soil columns. Soil Sci. 110:44–51.

van Genuchten, M. Th. 1980. A closed-form equation for predicting the hydraulic conductivity of unsaturated soils. Soil Sci. Soc. Am. J. 44:892–898.

van Genuchten, M. Th., and P. J. Wierenga. 1976. Mass transfer studies in sorbing porous media. I. Analytical solutions. Soil Sci. Soc. Am. J. 40:473–480.

Vanclooster, M., J. J. T. I. Boesten, M. Trevisan, C. D. Brown, E. Capri, O. M. Eklo, B. Gottesburen, V. Gouy, and A. M. A. van der Linden. 2000. A European test of pesticide-leaching model: Methodology and major recommendations. Agric. Water Manag. 44:1–19.

Vaughan, P. J., and D. L. Suarez. 2003. Constant capacitance model computation of boron speciation for varying soil water content. Vadose Zone J. 2:253–258.